

INTERNATIONAL UNION OF PURE
AND APPLIED CHEMISTRY
MACROMOLECULAR DIVISION
COMMISSION ON POLYMER CHARACTERIZATION
AND PROPERTIES
WORKING PARTY ON STRUCTURE AND PROPERTIES
OF COMMERCIAL POLYMERS*

**A COLLABORATIVE STUDY OF THE
STABILITY OF EXTRUSION, MELT
SPINNING AND TUBULAR FILM
EXTRUSION OF SOME HIGH-, LOW-
AND LINEAR-LOW DENSITY
POLYETHYLENE SAMPLES**

Prepared for publication by

JAMES L. WHITE and HIDEKI YAMANE

Polymer Engineering Center, University of Akron
Akron, Ohio, USA

*Membership of the Working Party during the preparation of this report (1983–85) was as follows:

Chairman: H. H. Meyer (FRG); *Secretary:* D. R. Moore (UK); *Members:* G. Ajroldi (Italy); R. C. Armstrong (USA); C. B. Bucknall (UK); J. M. Cann (UK); D. Constantin (France); H. Coster (Netherlands); Van Dijk (Netherlands); M. Fleissner (FRG); H.-G. Fritz (FRG); P. H. Geil (USA); A. Ghijsels (Netherlands); G. Goldbach (FRG); D. J. Groves (UK); H. Janeschitz-Kriegl (Austria); P. B. Keating (Belgium); H. M. Laun (FRG); A. S. Lodge (USA); C. Macosko (USA); J. Meissner (Switzerland); A. Michel (France); A. Plochocki (USA); W. Retting (FRG); K. P. Richter (FRG); G. Schorsch (France); G. Schoukens (Belgium); J. C. Seferis (USA); J. M. Starita (USA); G. Vassilatos (USA); J. L. White (USA); H. H. Winter (USA); J. Young (Netherlands); H. G. Zachmann (FRG).

Republication of this report is permitted without the need for formal IUPAC permission on condition that an acknowledgement, with full reference together with IUPAC copyright symbol (© 1987 IUPAC), is printed. Publication of a translation into another language is subject to the additional condition of prior approval from the relevant IUPAC National Adhering Organization.

A collaborative study of the stability of extrusion, melt spinning and tubular film extrusion of some high-, low- and linear-low density polyethylene samples

Abstract - A comparative study by several industrial and academic laboratories of the shear and elongational rheological behavior and unstable processing behavior of a series of well characterized linear and branched polyethylene is reported. The processing operations investigated were flow through a die, melt spinning and tubular film extrusion. Broadening molecular weight distribution in the linear polyethylenes increased deviations from Newtonian flow, increased elastic memory and decreased filament stability in elongational flow. It also deteriorated melt spinning stability but broadened the range of stable operation in tubular film extrusion. Extrudate distortion occurred at the same critical die wall shear stress, but the characteristics of the unstable region were changed. Long chain branched polyethylenes exhibited generally enhanced elastic memory, greater stability and deformation rate hardening in uniaxial extension. Melt spinning and tubular film extrusion characteristics were stabilized relative to linear polyethylenes, but extrudate distortion first occurred at a lower shear stress. The unstable extrusion characteristics were quite different from the linear polyethylenes. The linear low density polyethylene investigated generally responded similarly to a linear polyethylene of about the same molecular weight distribution.

INTRODUCTION

No commercial polymer is more important or has received the same attention as polyethylene. The rheological and melt processing behavior has been widely studied. Two previous major studies by this IUPAC Working Party have characterized the rheological and film blowing characteristics of low density and high density polyethylene (ref. 1,2).

The subject of instabilities is an important one to the polymer rheologist and process engineer. Four classes of instabilities have received considerable attention in the literature. These are instabilities in simple uniaxial extension of molten filaments (ref. 3,5), breakdown of stable drawdown of molten filaments/films during melt spinning of film casting (ref. 6-13), instabilities in tubular films extrusion behavior (ref. 13-16) and unstable extrusion (ref. 17-23). All of these phenomena occur to varying extents in commercial polyethylenes (ref. 3, 4, 13-16, 18-23). However, the extent and character of each seems to vary with the molecular weight, distribution of molecular weights and extent and types of long chain branching. While there have been individual studies of these instabilities, little effort has been made to make a joint study of them.

In the present paper, we describe a joint study of the rheological properties and melt flow instabilities using a series of molecularly well characterized polyethylenes, of varying molecular weight distribution, and extent and type of branching. This report describes the contributions of thirteen European and North American Laboratories, of which nine were industrial, three academic and one government. These organizations and the primary investigators are:

BASF AG Ludwigshafen, West Germany (BASF) H.M. Laun

Borg Warner Amsterdam, Netherlands (BW) H. Coster

BP Chemicals Ltd. Grangemouth, UK (BP) S.T.E. Aldhouse

CdF Chimie Bully des Mines, France (CdFC) D. Constantin

Eidgenossische Technische Hochschule, Zurich, Switzerland (ETH) J. Meissner

Hoechst AG Hoechst, West Germany (Hoechst) M. Fleissner

ICI Wilton, UK (ICI) D.J. Groves

Industrial Materials Research Institute Boucherville, Montreal, Canada (IMRI)
L.A. Utracki/P. Sammut

Koninklijke/Shell Laboratorium Amsterdam, Netherlands (Shell) A. Ghijsels

Montepolimeri Bollate, Italy (M) G. Ajroldi

Rheometrics Inc. New Jersey, USA/Frankfort, West Germany (Rheo) J.M. Starita/C. Frank

The University of Akron, Polymer Engineering Center, Akron, OH USA (APEC)
J.L. White/ Y. Yamane

The University of Massachusetts, Amherst, Mass., USA (UM) H.H. Winter

EXPERIMENTAL

Materials

A series of six polyethylenes were included in this study. This includes three high density polyethylenes (HDPE), two low density polyethylenes (LDPE) and a linear low density polyethylene (LLDPE). Two HDPE (HDPE-1, HDPE-2) were supplied by Hoechst and the third HDPE-3 by DuPont. The two LDPE were supplied by BP. The L-LDPE was supplied by CdF Chimie. The characteristics of these polymers are summarized in Table 1. According to Hoechst, HDPE-1 and HDPE-2 contain some butene-1 as a comonomer.

Molecular weight distribution of the samples were determined by BP, CdFC, Hoechst and Institute of Macromolecular Chemistry (IMC) of the Czechoslovak Academy of Science (IUPAC Subgroup IV-2.1.2) using gel permeation chromatography. The experimental conditions of GPC measurements are shown in Table 2. CdFC GPC traces for the polymers studied are contained in Fig. 1. The GPC was calibrated by polyethylene and polystyrene standards using Universal

TABLE 1. Characteristics of Polyethylenes Investigated

Symbol	Manufactured	Density (g/cm ³) (BASF)	Melt Index
HDPE-1	Hoechst	0.944-0.946	0.06
HDPE-2	Hoechst	0.939-0.942	0.45
HDPE-3	DuPont	0.950-0.953	
LLDPE	CdF Chimie	0.917-0.918	1.0
LDPE-1	BP	0.921	0.2
LDPE-2	BP	0.920-0.921	2.0

TABLE 2. Experimental Conditions for GPC Measurements

Laboratory	Solvent	Temperature	Concentration	Flow Rate
BP	1,2,4-Trichlorobenzene (TCB)	140°C	adjusted ($[\eta] \cdot C = 0.15$)	0.5 ml/min
CdFC	TCB	140°C	0.25%	1 ml/min
Hoechst	TCB	135°C	0.1 %	1 ml/min
IMC	o-dichlorobenzene	135°C	---	---

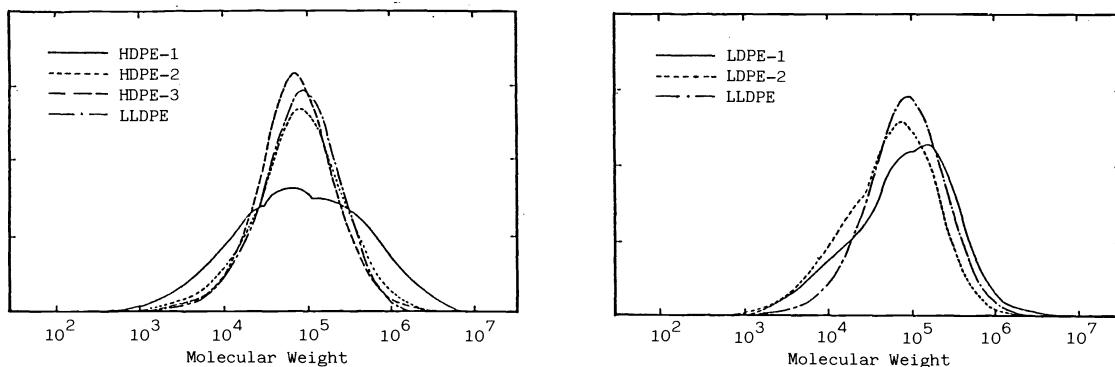


Fig. 1. GPC traces for polyethylenes

Calibration Curves. IMC made branching corrections for LDPE samples. The results are summarized in Table 3. The weight average molecular weights M_w of linear polyethylenes orders as:

HDPE-1 >> HDPE-2 > LLDPE > HDPE-3 (BP)
 HDPE-1 >> HDPE-2 > LLDPE > HDPE-3 (CdFC)
 HDPE-1 >> HDPE-2 >> LLDPE > HDPE-3 (Hoechst)
 HDPE-1 >> LLDPE > HDPE-2 > HDPE (IMC)

M_w/M_n order as:

HDPE-1 >> HDPE-2 > HDPE-3 ~ LLDPE (BP)
 HDPE-1 >> HDPE-2 > LLDPE > HDPE-3 (CdFC)
 HDPE-1 >> HDPE-2 >> LLDPE ~ HDPE-3 (Hoechst)
 HDPE-1 >> HDPE-2 > LLDPE > HDPE-3 (IMC)

where the double inequality in all cases indicates a factor of about two or more. HDPE-1 has a large high molecular weight tail, and HDPE-2 a more modest one.

Intrinsic viscosities, $[\eta]$ were obtained on all of the polyethylene samples in decahydronaphthalene at 130°C (IMC). The $[\eta]$ were converted to viscosity average molecular weight using the expression

$$[\eta] = 4.60 \times 10^{-2} \cdot M_{\eta}^{0.73} \quad (1)$$

The crystallinities of the samples have been estimated by Hoechst from infra red. The results are summarized in Table 4. The HDPE-2 has a crystalline fraction of 0.63 as opposed to the 0.67 value of HDPE-1 and HDPE-3. The LLDPE and LDPE-2 have values of 0.45, while LDPE-1 has the lowest value of 0.43.

Hoechst characterized branching in the polyethylenes using infra red absorption and BP carried out similar investigations with C 13 nuclear magnetic resonance. The results are contained in Tables 5 and 6. These generally show that the HDPE-3 has the lowest level of branching. The HDPE-1 and HDPE-2 have some ethyl branches as expected. The LLDPE has very significant levels of ethyl branches, an order of magnitude or higher levels than HDPE-1 or HDPE-2. The LDPE-1 and LDPE-2 have levels of total CH_3 about the same as LLDPE but the distribution of branch lengths is greater. The difference in branching of the LDPE-1 and LDPE-2 are not clear.

Shear flow

Rheological characterization

The rheological properties of the polymer melts have been characterized using different experimental techniques. Measurements of the shear viscosity were carried out variously in cone-plate and capillary rheometers. Rheo and APEC measured the viscosity as a function of shear rate in a Rheometrics System 4 and a Mechanical Spectrometer at 190°C. The measurements by APEC were carried on an instrument in the laboratories of Rheometrics. BP made measurements in a Rheometrics System 4 at 180°C. BW made studies in a Weissenberg Rheogoniometer at 170°C. Capillary rheometer experiments to determine viscosity were reported by BASF, CdFC, Hoechst, ICI, IMRI, and APEC at 190°C.

Principal normal stress difference N_1 measurements were made using a cone-plate geometry by BP and Rheo.

Linear viscoelastic oscillatory measurements

Measurements of dynamic viscosity $\eta'(\omega)$ and storage modulus $G'(\omega)$ were made by BW, CdFC, IMRI and Rheo at 190°C as well as by BW at 170°C and by Rheo at 150°C. The instruments used were a Rheometrics Dynamic Spectrometer with a pair of parallel plate of 1.25 cm in diameter and a Weissenberg Rheogoniometer with cone-plate mode (BW), a Contraves Kepes Balance Rheometer (CdFC), a Rheometrics Mechanical Spectrometer (IMRI) and a Rheometrics System 4 (Rheo).

Stress relaxation measurements following shear flow were made by BW at 170°C using an R18 Weissenberg Rheogoniometer and at 190°C following sudden strain with a Rheometrics Dynamic Spectrometer.

Elongational flow experiments

Uniaxial extension experiments were carried out in several laboratories including BASF, Hoechst, IMRI, Rheo, Shell and APEC. The apparatus and experiments are described below.

BASF made measurements at constant deformation rate in an elongational rheometer at 150°C.

TABLE 3. Molecular weight distributions based on GPC and $[\eta]$

Material	$M_n \times 10^{-3}$	$M_n \times 10^{-3}$	$M_w \times 10^{-3}$	$M_z \times 10^{-3}$	M_w/M_n	M_z/M_w	$[\eta]$	Laboratory
HDPE-1	13	—	332	—	26	—	—	BP
	20	—	315	1550	18	4.9	—	CdFC
	15	291	501	—	34	—	3.35	Hoechst
	11	—	274 (420)	—	25	—	2.58	IMC
HDPE-2	19	—	145	—	7.7	—	—	BP
	29	—	169	713	7.5	4.2	—	CdFC
	20	160	251	—	12	—	2.5	Hoechst
	18	—	119 (235)	—	6.6	—	2.03	IMC
HDPE-3	26	—	91	—	3.6	—	—	BP
	38	—	129	415	3.4	3.2	—	CdFC
	29	77	91	—	3.1	—	1.95	Hoechst
	16	—	80 (95)	—	5.0	—	1.46	IMC
LLDPE	33	—	113	—	3.4	—	—	BP
	36	—	143	356	3.9	2.5	—	CdFC
	34	94	110	—	3.2	—	1.67	Hoechst
	20	—	124 (127)	—	6.2	—	—	IMC
LDPE-1	17	—	128	—	7.6	—	—	BP
	25	—	190	836	7.5	4.4	—	CdFC
	—	—	—	—	—	—	1.30	Hoechst
	12	—	395 (560)	—	33	—	1.11	IMC
LDPE-2	15	—	77	—	5.0	—	—	BP
	22	—	114	431	5.2	3.8	—	CdFC
	—	—	—	—	—	—	1.05	Hoechst
	11	—	305 (219)	—	28	—	0.89	IMC

TABLE 4. Estimates of Crystallinity by Hoechst

Sample	Crystallinity
HDPE-1	0.67
HDPE-2	0.63
HDPE-3	0.67
LLDPE	0.45
LDPE-1	0.43
LDPE-2	0.45

TABLE 5. Infra Red Analysis of Branching of Hoechst

Sample	Total CH ₃ 1000C	Ethyl 1000C
HDPE-1	3.4	1.2
HDPE-2	3.2	1.6
HDPE-3	<2	<0.2
LLDPE	21.6	13.6
LDPE-1	25.0	6.5
LDPE-2	26.5	5.1

TABLE 6. C 13 Nuclear Magnetic Resonance Analysis of Branching by BP

Sample	Methyl 1000C	Ethyl 1000C	1,3-Diethyl 1000C	Butyl 1000C	Pentyl 1000C	Longer than C ₆ 1000C
HDPE-1	--	--	---	--	--	2.2
HDPE-2	--	--	---	--	--	1.1
HDPE-3	--	--	---	--	--	---
LLDPE	--	18.0	1.5	--	--	1.3
LDPE-1	4.2	1.4	0.5	7.4	2.5	3.1
LDPE-2	0.7	5.0	0.9	6.0	2.2	3.2

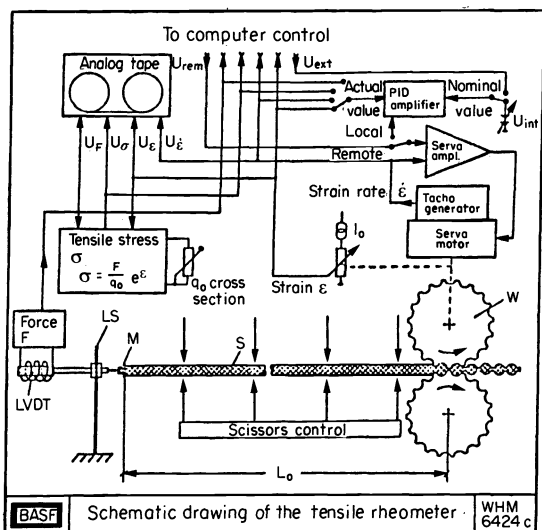


Fig. 2. Elongational flow apparatus of BASF

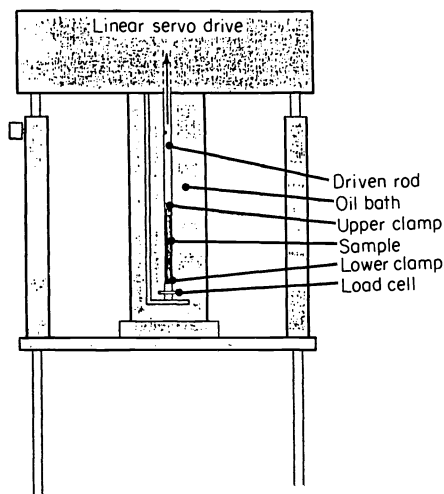


Fig. 3. Rheometrics extensional rheometer

The rod-like sample was prepared by extrusion. It was floated on silicone oil in a bath with electrically heated walls. Fig. 2 shows a schematic drawing of the rheometer. It has been described by Laun and Munstedt (ref. 24). A pair of toothed wheels (W) is used to stretch the sample (S) and the other end of the sample is glued to a metal strip (M) that is connected to the leaf spring of a force transducer. To check homogeneity of sample deformation and to determine the recoverable strain, the sample is cut by means of scissors after a given total strain. Local control of the apparatus was used and a constant Hencky strain rate imposed by a constant rotary speed of the servo motor.

Hoechst, IMRI, Rheo and Shell made experiments with a Rheometrics Extensional Rheometer (see Fig. 3). The specimens to be stretched in this experiment are prepared by compression molding. The measurements of Hoechst and Rheo were at 150°C, those of Shell at 190°C.

APEC made experiments on an apparatus newly developed by H. Yamane in its laboratories (see Fig. 4). It is similar in design to the BASF instrument described above and is based on upgrading of an instrument originally described by Yamane and White (ref. 25). The specimens were prepared by extrusion.

ICI measured elongational viscosities using die entrance pressure drops. These were computed using the theory of Cogswell (ref. 26).

Equal biaxial extension measurements followed by stress relaxation were carried out by UM in a Rheometrics RDS-LA rheometer using lubricated squeezing silicone oils (General Electric Viscasil) were used as the lubricants. This is illustrated in Fig. 5.

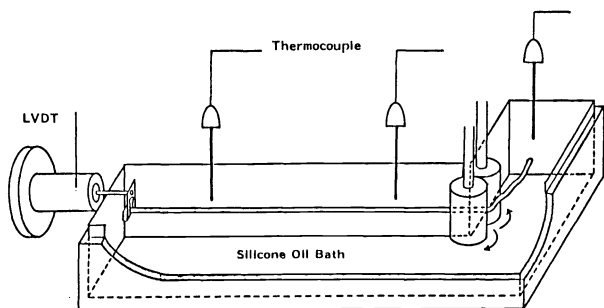


Fig. 4. APEC elongational flow rheometer

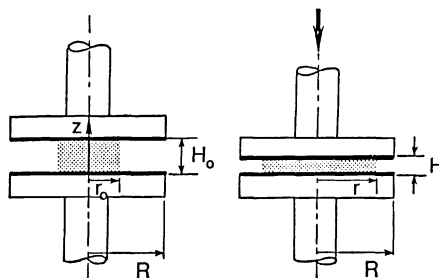


Fig. 5. UM lubricated squeezing flow experiments

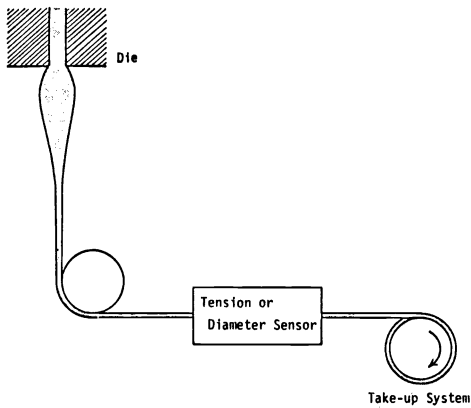


Fig. 6. Melt spinning experiments

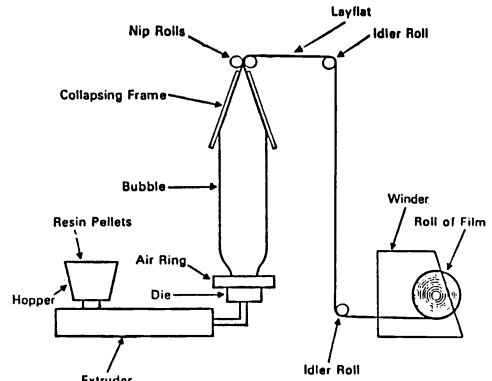


Fig. 7. Tubular blown film extrusion experiments of APEC

Melt spinning (Fig. 6)

Melt spinning experiments were carried out by BP, CdFC, Hoechst, Shell and APEC. The experimental procedures are described below.

BP used a Goettfert Rheotens apparatus which measures the take-up velocity, v_L , and spinline tension F . The melt temperature was 180°C . The spinline was not thermostatted. The spinline length from the die face to the axes of the take-up rollers was 121 mm. Tests were conducted at output rates from 130 to 530 mm^3/sec . The take-up speed was changed continually. The rate of change of take-up was kept low and did not affect the results.

CdFC used a Toyoseiki melt tension tester, which is a ram extruder with a tension measuring take-up device. A die of diameter 2 mm. and L/D ratio of 4 was used. The melt temperature was 190°C . The spinline which was not thermostatted had a length 250 mm. The extrusion rate was $11.8 \text{ mm}^3/\text{sec}$. Experiments were carried out at constant take-up speed which was then increased by step.

Shell carried out melt spinning experiments with a Goettfert single screw laboratory extruder with a screw diameter of 20 mm and length of 40 mm. A capillary die of diameter 3 mm. L/D of 10 and 90° entrance angle was used. The melt temperature was 190°C . Most experiments were carried out under non-isothermal conditions (cooling of extrudate by ambient air). The spinline length was 180 cm. and the mass flow rate 10 g/min . ($219.3 \text{ mm}^3/\text{sec}$). The filaments were drawn down using a Goettfert Rheotens. One series of experiments was carried out with steadily increasing take-up velocity (acceleration = $1.2 \text{ mm}/\text{sec}^2$). Another series was performed at constant take-up speed conditions so as to measure the extent of draw resonance under steady conditions. These experiments were started at low speeds which was then increased in steps into the region where draw resonance occurs. At each take-up speed, the diameter of the spinline at the position of the take-up wheels was continuously measured by an optical laser technique. Both the amplitude and the periodicity of the instabilities were taken from these diameter data when a steady state pulsation of the diameter was obtained.

APEC carried out melt spinning experiments with an Instron Capillary Rheometer. A capillary die of diameter 0.147 cm and L/D of 28 was used for non-isothermal melt spinning, and another die of diameter 0.107 cm and L/d of 29 was used for isothermal runs. For isothermal melt spinning, an isothermal chamber was attached to the bottom of the barrel of the Instron Capillary Rheometer to keep the temperature of the spinline air the same as polymer melt temperature (Fig. 4). The distance between the die exit to the surface of the quench water were 7 cm in the isothermal case and 2.5 cm in the non-isothermal case. The flow rates were $9.05 \times 10^{-4} \text{ cm}^3/\text{sec}$. for both cases.

Tubular film extrusion

Tubular film extrusion experiments were carried out by APEC. A $\frac{3}{4}$ inch Killion Screw Extruder with tubular die and frame was used. An annular die of outer radius 3.175 cm. and gap of 0.1 cm. was used. An extrusion rate of $1500 \text{ cm}^3/\text{hr}$ was used in all of the experiments. The melt temperature in the die was held as close to 190°C as possible. This is illustrated in Fig. 7.

Extrusion instabilities

Extrusion instabilities, notably extrudate distortion have been investigated by BASF, CdFC, ETH, M and APEC. BASF, ETH and M used Goettfert a Rheograph 2000 which has a barrel diameter of $\frac{3}{8}$ inch. A Dynisco pressure transducer was placed at the capillary inlet. BASF used circular dies of diameter 0.5 mm to 2.5 mm and L/D ratio of 30. M used two dies with diameter 1 mm and L/D ratio of 0 and 30. APEC used a Monsanto Processability Tester with a die of diameter 0.762 mm and L/D = 30. CdFC and Brabender extrusion screw extruder with dies of diameter 1.02 to 3 mm.

SHEAR VISCOSITY MEASUREMENTS

Results

Many Laboratories (CdFC, MP, Rheo, APEC) reported shear viscosity data at 190°C. These are summarized in Figure 8 together with data of BP determined at 180°C. The data have great qualitative similarities. The viscosity for all of the polyethylenes exhibits a plateau of low shear rates and then decreases with increasing rates of shear. The magnitudes of the plateaus and rates of decrease change from material to material. The data at a shear rate of 10^{-2} sec $^{-1}$ order as

$$\text{HDPE-1} > \text{LDPE-1} > \text{HDPE-2} > \text{LLDPE} > \text{LDPE-2} > \text{HDPE-3}$$

At a shear rate of 100 sec $^{-1}$, the curves have re-ordered with

$$\text{HDPE-1} \sim \text{HDPE-2} \sim \text{LLDPE} > \text{LDPE-1} \sim \text{HDPE-3} > \text{LDPE-2}$$

There are differences in the data from the individual laboratories. Generally the results of BP tend to be higher and CdFC lower in the low shear rate region. This should not be unexpected of the BP data as the measurements were performed at 180°C.

Interpretation

The viscosity function is well known to be related to molecular weight and its distribution (ref. 5, 25, 27, 28). In Table 7, we summarize zero shear viscosity of the polyethylenes studied as a fraction as function of weight average molecular weight. It may be seen that the values of η_0 for the LDPEs fall below the HDPEs and LLDPEs at specific M_w . The data on the latter two polymers are roughly consistent. This effect has been noted by earlier investigators (ref. 29, 30) studying the zero shear viscosities of linear and branched polyethylenes.

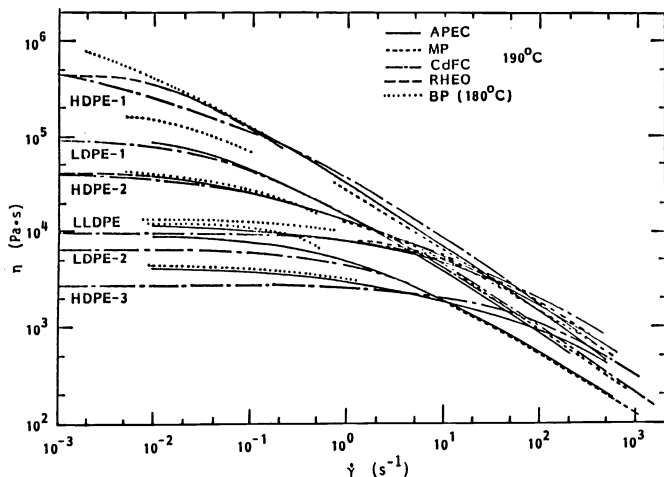


TABLE 7. Zero shear viscosities as a function of weight average molecular weight from polyethylenes studies

Polymer	$M_w \times 10^{-3}$		$\eta_0 \times 10^{-4}$ (Pa · S)
	CdFC	Hoechst	
HDPE-1	315	501	>60
HDPE-2	169	251	3.97
HDPE-3	129	91	0.41
LLDPE	143	110	1.16
LDPE-1	190	---	9.70
LDPE-2	114	---	0.93

Fig. 8. Shear viscosity η of polyethylenes as a function of shear rate $\dot{\gamma}$ at 190°C

The shear rate dependence of the viscosity function is widely considered to be related to the breadth of the molecular weight distribution in linear polymer system. In Figure 9, we construct a Vinogradov-Malkin plot (ref. 28) of η/η_0 vs. $\eta_0 \dot{\gamma}$ for the HDPE-1, HDPE-2, and the HDPE-3. The LLDPE which is also a linear polymer is included. Generally the rate of 'fall off' of the data orders as

$$\text{HDPE-1} > \text{HDPE-2} > \text{HDPE-3} \sim \text{LLDPE}$$

which corresponds to the breadth of the molecular weight distribution. The data may be compared with earlier correlations of this type by Yamane, Minoshima and White (ref. 13, 25).

A similar η/η_0 plot for the LLDPE, LDPE-1 and LDPE-2 is given in Fig. 10.

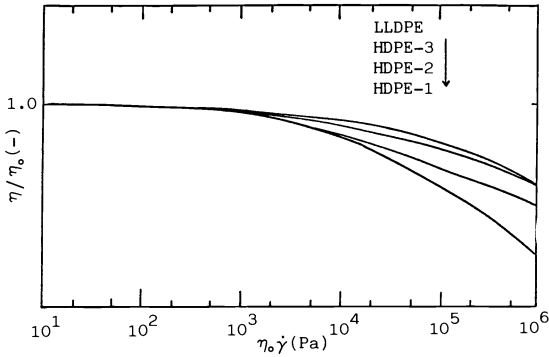


Fig. 9. Reduced viscosity η/η_0 as a function of $\eta_0 \dot{\gamma}$ for HDPE-1, HDPE-2, HDPE-3 and LLDPE (CdFC)

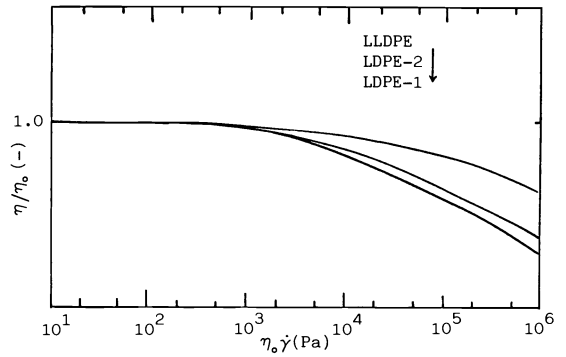


Fig. 10. Reduced viscosity η/η_0 as a function of $\eta_0 \dot{\gamma}$ for LDPE-1, LDPE-2 and LLDPE (CdFC)

PRINCIPAL NORMAL STRESS DIFFERENCE MEASUREMENTS

Results

The principal normal stress differences N_1 of the melts were reported by Rheo and BP. Rheo's measurements are presented in Fig. 11 as a function of shear stress. This type of plot has been found by earlier researchers (ref. 5, 29, 30) to be independent of temperature and sensitive to molecular weight distribution. As shown by Coleman and Markovitz (31) at low shear stresses N_1 is related to shear stress as

$$N_1 = 2 J_e \sigma_{12}^2 \tag{2}$$

Estimated values of J_e are summarized in Table 8. The data order as

$$LDPE-1 > LDPE-2 > HDPE-2 > LLDPE > HDPE-1$$

The results of BP were obtained on a parallel plate instrument. ψ_1 , the principal normal stress difference coefficient was estimated. This was converted to J_e and the values are also summarized in Table 8. BP could not obtain steady state data on HDPE-1 or LDPE-1. The J_e data order as

$$LDPE-2 > HDPE-2 > LLDPE > HDPE-3$$

The Rheo and BP data are qualitatively consistent but differ quantitatively.

At high shear rates instabilities develop in this instrument and the melt emerges from the gap.

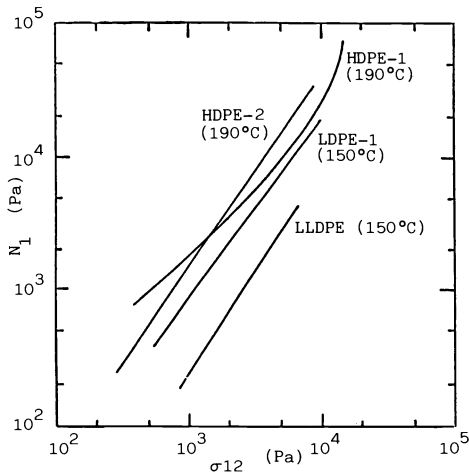


Fig. 11. Principal normal stress difference N_1 as a function of shear stress σ_{12} for polyethylenes (Rheo)

TABLE 8. Steady State Compliance and Relaxation Time for Polyethylene Samples (BP, Rheo)

Material	J_e (Pa) $\times 10^5$	J_e (Pa) $\times 10^5$	J_e (Pa) $\times 10^5$	$\bar{\tau}$ (sec)
	(BP) Normal Stress	(Rheo) Normal Stress	(Rheo) Dynamic	
HDPE-1	---	0.22	0.9	40.5
HDPE-2	0.299	0.96	1.5	6.0
HDPE-3	0.132	---	---	---
LLDPE	0.283	0.54	1.1	1.06
LDPE-1	---	1.7	1.6	14.4
LDPE-2	0.719	0.99	2.1	1.85

Discussion

Rheo's data indicate that the steady state compliance and memory of LDPE-1 is greater than that of the other melts. The values for LDPE-2 are second in magnitude. From BP the HDPE-3 has the lowest J_e followed by LLDPE. This indicates the highest values are for the long chain branched polyethylenes and the narrow molecular weight distribution linear polymers possess the lowest values. This is similar to earlier results for polyolefins (ref. 11-13, 16). The low value $\delta f J_e$ for the broad distribution HDPE-1 is surprising.

The mean relaxation time $\bar{\tau}$ was determined by Rheo from

$$J_e \eta_0 = \bar{\tau} \quad (3)$$

This is summarized in Table 8. The data order as

$$\text{HDPE-1} > \text{LDPE-1} > \text{HDPE-2} > \text{LDPE-2} > \text{LLDPE}$$

LINEAR VISCOELASTIC MEASUREMENTS

Results

Dynamic viscosity $\eta'(\omega)$ and storage modulus $G'(\omega)$ data have been reported by BW, CdFC, IMRI and Rheo as a function of frequency. $\eta'(\omega)$ and $G'(\omega)$ are plotted as a function of frequency in Fig. 12 and 13. The complex viscosity η^* defined by

$$\eta^* = \sqrt{(\eta')^2 + (G'/\omega)^2} \quad (4)$$

is plotted as a function of frequency in Fig. 14 for experiments carried out at 190°C. At low frequencies, the η' and η^* data order as

$$\text{HDPE-1} > \text{LDPE-1} > \text{HDPE-2} > \text{L-LDPE} > \text{LDPE-2} > \text{HDPE-3}$$

At a frequency of 100 sec^{-1} , the $\eta^*(\omega)$ data order as

$$\text{HDPE-2} > \text{L-LDPE} > \text{HDPE-1} > \text{HDPE-3} > \text{LDPE-1} > \text{LDPE-2}$$

BW also presents data at 170°C which order in the same manner.

The storage modulus G' data at 190°C is presented in Fig. 13 at a frequency of 10^{-1} sec^{-1} . The data order as

$$\text{HDPE-1} > \text{LDPE-1} > \text{HDPE-2} > \text{L-LDPE} > \text{LDPE 2} > \text{HDPE-3}$$

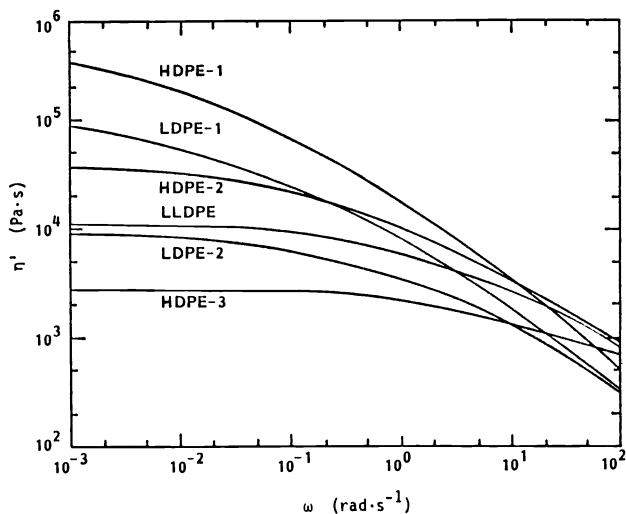


Fig. 12. Dynamic viscosity $\eta(\omega)$ at 190°C for polyethylene melts as a function of frequency ω (CdFC)

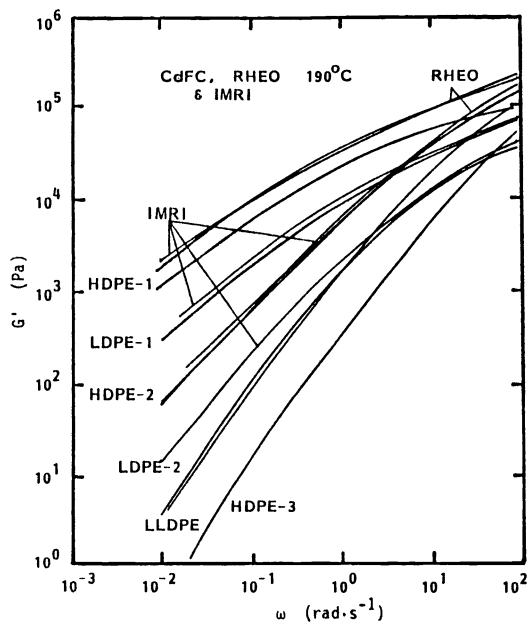


Fig. 13. Storage modulus $G'(\omega)$ at 190°C for polyethylene melts as a function of frequency ω (Rheo, CdFC and IMRI)

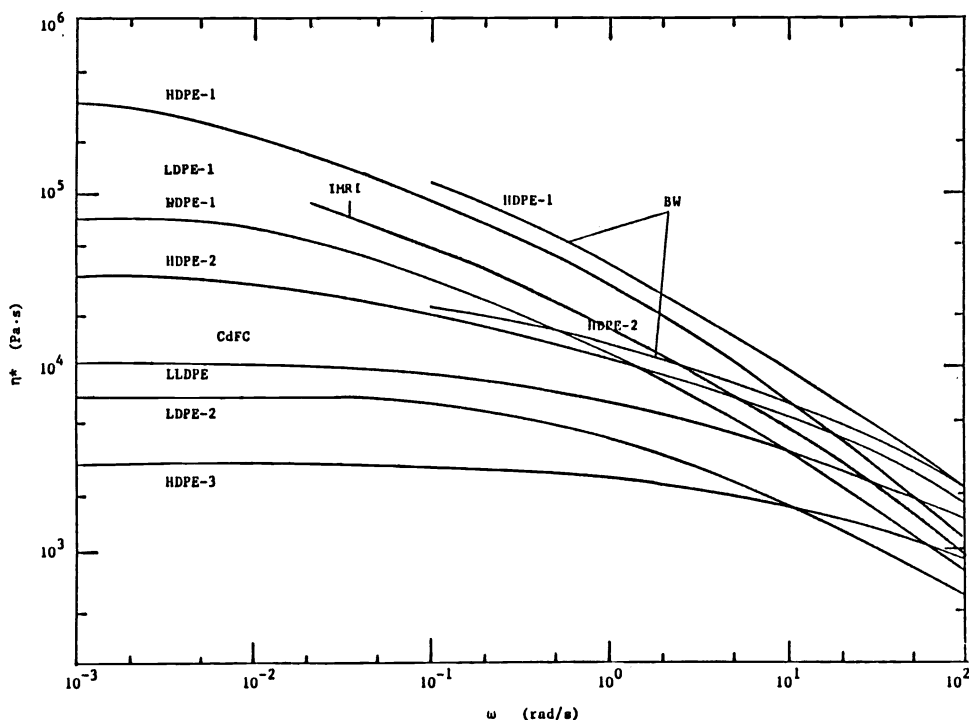


Fig. 14. Complex viscosity η^* of polyethylene melts as a function of frequency ω . (CdFC and BW)

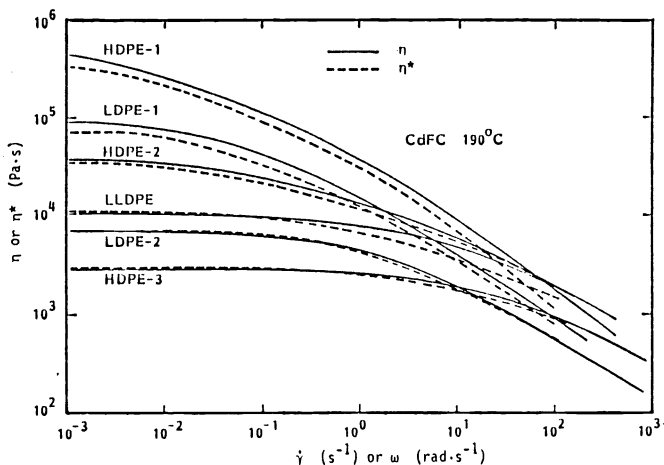


Fig. 15. Test of Cox-Merz relationships between $\eta(\dot{\gamma})$ and $\eta^*(\omega)$ (CdFC)

Discussion

The Cox-Merz (ref. 32) empirical relationship connecting the complex viscosity $\eta^*(\omega)$ and the shear viscosity $\eta(\dot{\gamma})$ appears to work rather well at lower shear rates especially if the data of the same laboratory, e.g. CdFC, is used for each function. A comparison is made in Fig. 15. At higher shear rates deviations are observed especially for the LLDPE.

J_e was computed from $G'(\omega)$ and $\eta'(\omega)$ by Rheo through the approximate relationship

$$J_e = \frac{G'}{(\omega \eta')^2} \Bigg|_{\omega = 0.1 \text{ sec}^{-1}} \tag{5}$$

The results are summarized in Table 8. The results order as

$$LDPE-2 > LDPE-1 > HDPE-2 > LLDPE > HDPE-1$$

which agree roughly qualitatively with those of the Rheo normal stress results but not in absolute magnitudes. The long chain branched LDPEs have the highest J_e and the narrow molecular weight distributions linear polyethylenes the lowest.

UNIAXIAL ELONGATIONAL FLOW

Results

Elongational flow characteristics of the various melts studied have been reported by BASF, Hoechst, IMRI, Rheo, Shell and APEC. BASF using a rheometer built in their laboratories presents steady state elongational viscosities determined by BASF are plotted in Fig. 16. APEC carried out the elongational flow experiments on their apparatus (Fig. 4) at 190°C. Their results are shown in Figure 17.

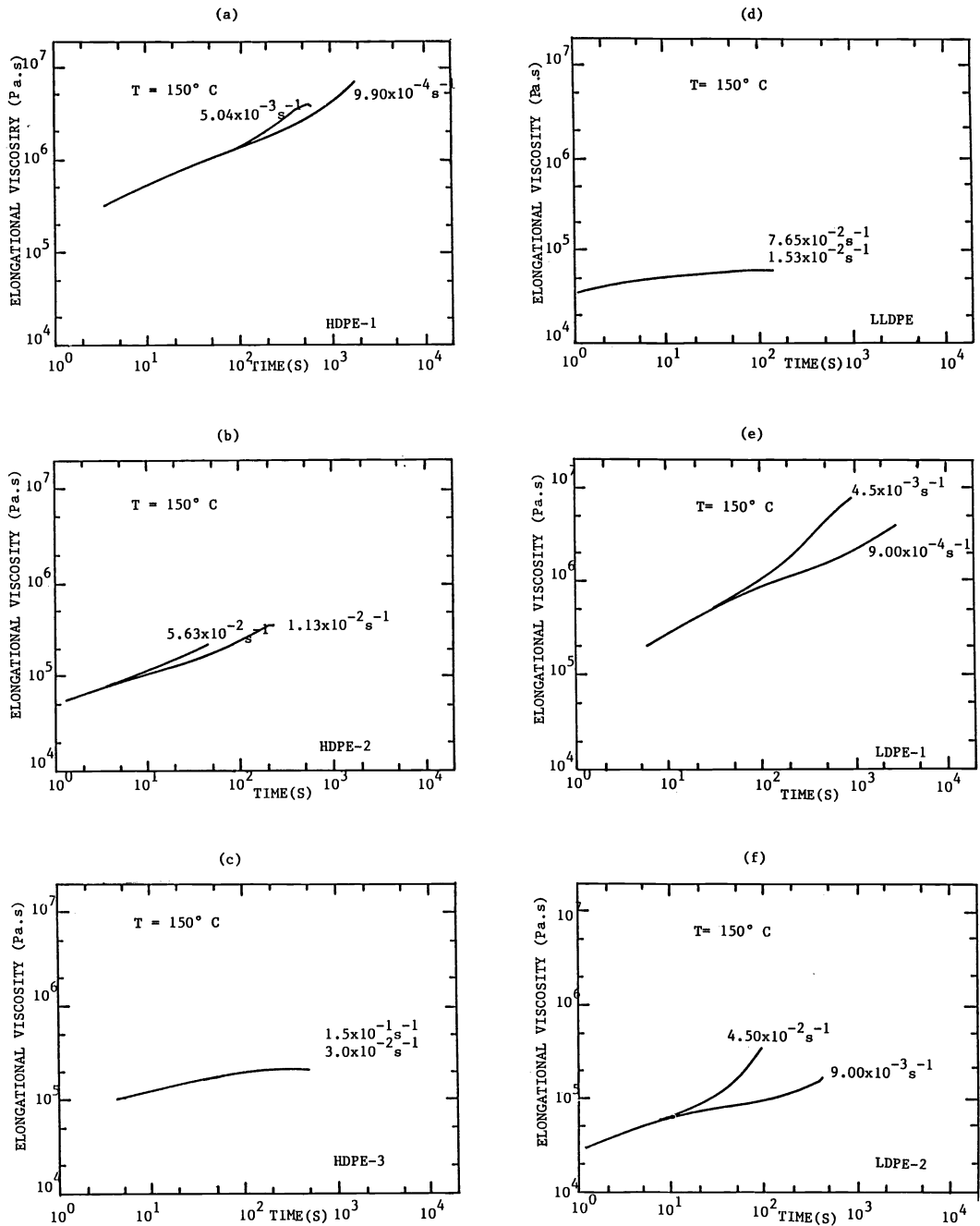


Fig. 16. Transient elongational viscosity $\chi(t)$ for polyethylene melts as a function of time t at 150°C (BASF)

- a) HDPE-1 b) HDPE-2 c) HDPE-3
 d) LLDPE e) LDPE-1 f) LDPE-2

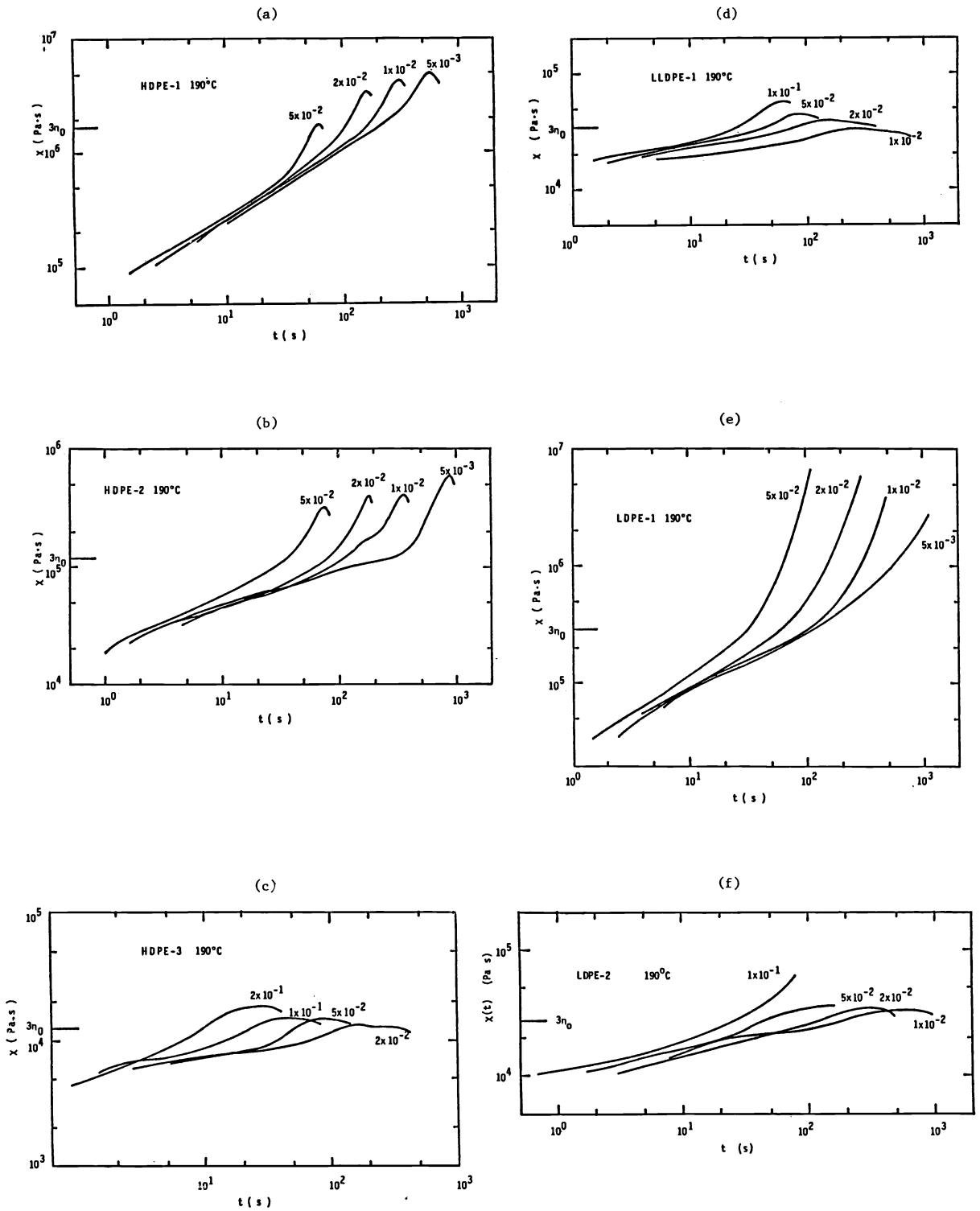


Fig. 17. Transient elongational viscosity $X(t)$ for polyethylene melts as a function of time t at 190°C (APEC)

- a) HDPE-1 b) HDPE-2 c) HDPE-3
- d) LLDPE e) LDPE-1 f) LDPE-2

Elongational flow data on a Rheometrics Extensional Rheometer are given by Hoechst, IRMI, Rheo and Shell. Typical data of Hoechst at 150°C and IMRI (150°C, 190°C) are shown in Fig. 18 and Fig. 19.

The materials respond as three different groups. The HDPE-3 and LLDPE show slow buildups of elongational viscosity to a steady state value. Their steady state elongational viscosities are essentially Newtonian being equal to $3\eta_0$. The LDPE-1 and LDPE-2 especially the former are strain hardening. The broader molecular weight distribution HDPE-1 and HDPE-2 do not appear to achieve steady states.

The elongations to break from the Shell and APEC data are listed in Table 9. The values for HDPE-1 and HDPE-2 are lower than for the other melts.

ICI concluded using entrance pressure losses that HDPE-1, HDPE-2, HDPE-3 and LLDPE all exhibited decreasing elongational viscosities.

Discussion

It seems clear that the LDPE-1 and LDPE-2 are strain hardening and show increasing elongational viscosities while HDPE-3 and LLDPE are nearly linear viscoelastic. The LDPE-1 and LDPE-2 are the most stable filaments and the HDPE-1 and HDPE-2 seem the most unstable in uniaxial elongational flow. This in agreement with early studies for similar materials (ref. 13, 16) and studies for the polyolefins (ref. 11,12)

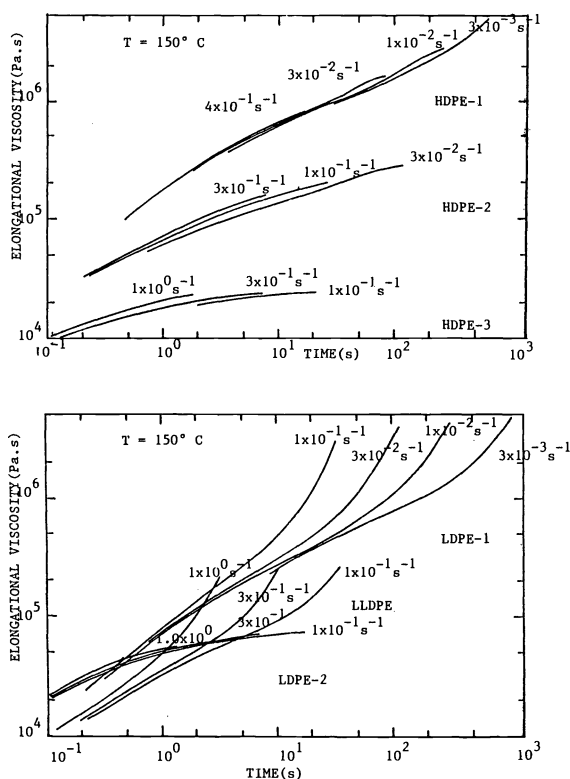


Fig. 18. Transient elongational viscosity $\chi(t)$ for polyethylene melts as a function of time at 150°C on Rheometrics Extensional Rheometer (Hoechst)

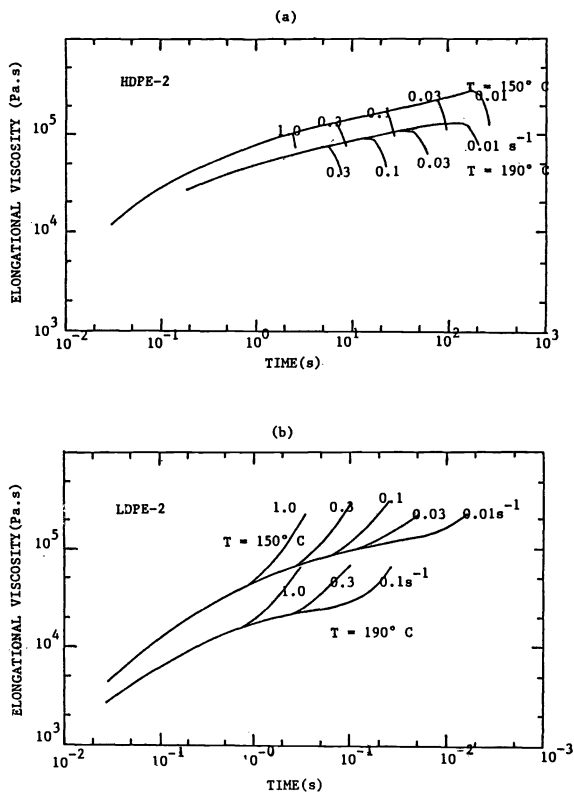


Fig. 19. Transient elongational viscosity $\chi(t)$ for polyethylene melts as a function of time t at 150°C and 190°C IMRI

TABLE 9. Hencky Strains to Failure of Polyethylene Filaments

Polymers	Stretch Rate (sec ⁻¹)	Shell	APEC	Polymers	Stretch Rate (sec ⁻¹)	Shell	APEC
HDPE-1	0.005		3.4	LLDPE	0.01		7.9
	0.01		3.0		0.02		7.4
	0.02		2.9		0.05		7.5
	0.05		3.0		0.10		7.4
	0.25	2.5			0.25	>3	
	0.50	2.5			0.50	>3	
	1.00	1.55			1.00	>3	
HDPE-2	0.005		5.3	LDPE-1	0.005		6.6
	0.01		3.7		0.01		6.0
	0.02		3.8		0.02		5.7
	0.05		4.0		0.05		5.6
	0.25	1.2			0.25	>3	
	0.50	1.6			0.50	>3	
	1.00	1.6			1.00	>3	
HDPE-3	0.02		8.0	LDPE-2	0.01		9.5
	0.05		7.9		0.02		8.7
	0.10		8.2		0.05		8.2
	0.20		8.3		0.10		7.6
	0.25	>3			0.25	>3	
	0.50	>3			0.50	>3	
	1.00	>3			1.00	>3	

MULTIAXIAL ELONGATIONAL FLOW

The six polyethylene samples were strained to varying amounts H/H₀ of 0.6 and 0.2 and the relaxation rates followed. Typical results are shown in Fig. 20. Generally the high density polyethylenes show greater strain dependence of the stresses (moduli). Relaxation times were determined from the data. These are summarized in Table 10. They order as

- HDPE-1 > HDPE-2 > HDPE-3 (190°C)
- LDPE-1 > LDPE-2 > LLDPE (150°C)

TABLE 10. Relaxation Times τ_B from Biaxial Elongation flow Experiment of UM

Material	Temperature (°C)	τ_B (sec) at $\epsilon_b = 0.26$
HDPE-1	190°	59.3
HDPE-2	190°	22.3
HDPE-3	190°	3.26
LLDPE	150°	10.2
LDPE-1	150°	52.0
LDPE-2	150°	23.3

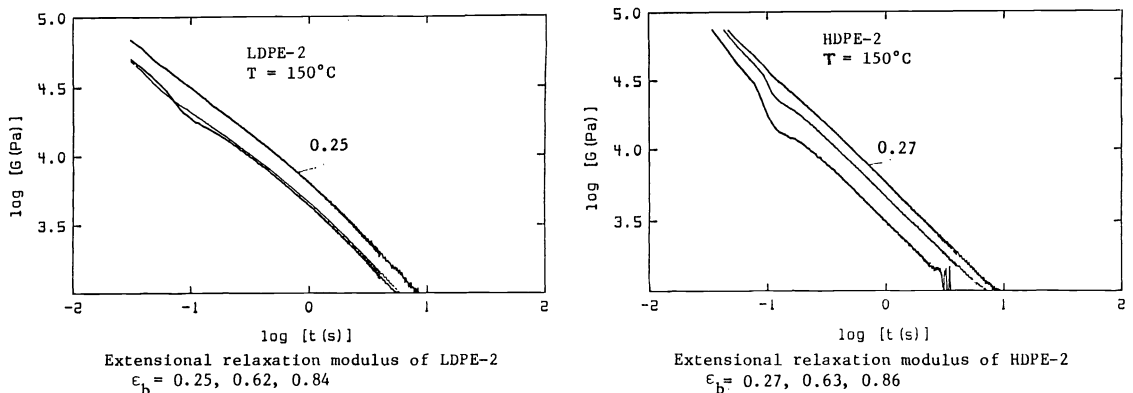


Fig. 20. Typical results of biaxial elongational flow and relaxation (UM)

MELT SPINNING

Results

The melt spinning of the various polymers included in this study have been investigated by BP, CdFC, Hoechst, Shell and APEC. The studies of BP and CdFC concentrate on stable melt spinning behavior.

First we will summarize the research results on Shell. In Fig. 21, we plot spinline tension as a function of drawdown ratio. It can be seen that the tension at low drawdown ratios V_L/V_0 exhibits small diameter fluctuations. At a roughly critical value of V_L/V_0 , the amplitudes become much larger in magnitude. The actual amplitude of the diameter fluctuations is plotted in Fig. 22. The growth in amplitude is sudden and large in magnitude. The critical values are summarized in Table 11. The materials studied order in terms of increasing stability

$$\text{LDPE-2} > \text{HDPE-3} > \text{LDPE-1} > \text{LLDPE} > \text{HDPE-2} > \text{HDPE-1}$$

The diameter oscillations are periodic in character. The resonance period and wavelength are summarized in Table 12. The resonance period is independent of drawdown ratio and orders as

$$\text{HDPE-2} > \text{LLDPE} \sim \text{HDPE-3} > \text{HDPE-1} > \text{LDPE-1} \sim \text{LDPE-2}$$

The experimental results of APEC generally correspond to those of Shell. The ordering of the stability differs with respect to HDPE-3, LLDPE and LDPE-1. The specific numbers are tabulated in Table 13. Another difference is that APEC finds that LDPE-2, the most stable material, much more resistant to draw resonance than Shell. Summarizing,

$$\text{LDPE-2} > \text{LDPE-1} > \text{LLDPE} > \text{HDPE-3} > \text{HDPE-2} > \text{HDPE-1}$$

Hoechst and Shell drawdown the filaments in the spinline until the filaments break. The spinline rupture data is summarized in Table 13. The extensibility to rupture orders as:

$$\text{LDPE-2} > \text{HDPE-3} > \text{LDPE-1} > \text{LLDPE} > \text{HDPE-2} > \text{HDPE-1}$$

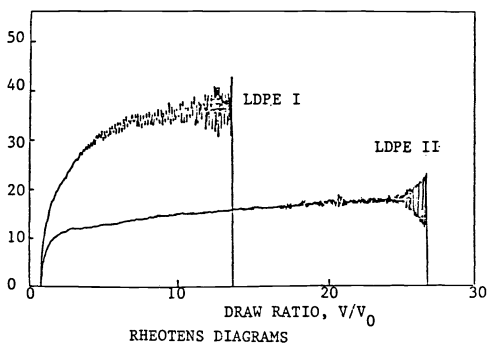
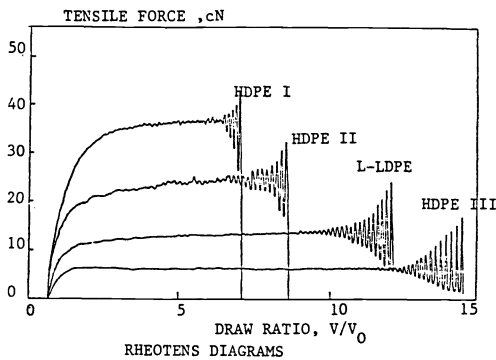


Fig. 21. Spinline tension as a function of drawdown ratio (Shell)

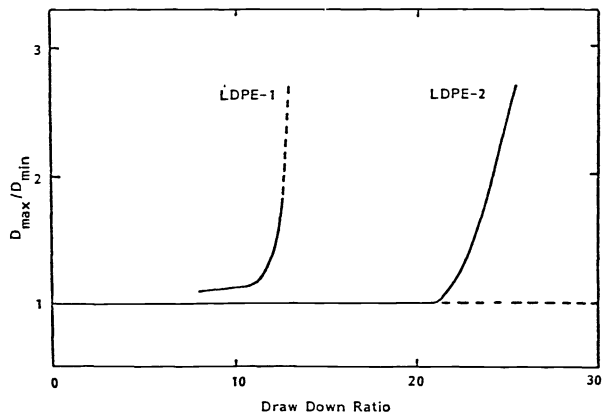
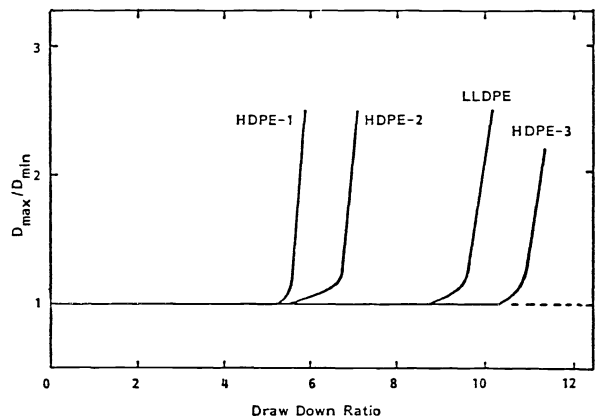


Fig. 22. Amplitude of diameter fluctuations as a function of drawdown ratio (Shell)

TABLE 11. Critical Drawdown Ratios for onset of Draw Resonance

Material	Shell	APEC
HDPE-1	5.6	4.9
HDPE-2	6.8	6.7
HDPE-3	10.5	10.9
LLDPE	9.3	11.7
LDPE-1	11.2	15.1
LDPE-2	23.2	45.0

TABLE 13. Spinline Rupture Data

Material	σ (MPa)	Shell		Hoechst
		V_L/V_0	V_L/V_0	V_L/V_0
HDPE-1	0.38	7.0	6.4	
HDPE-2	0.30	8.5	8.5	
HDPE-3	0.14	14.6		
LLDPE	0.24	12.0	11.8	
LDPE-1	0.70	13.3	13.2	
LDPE 2	0.60	26.4	>26.3	

TABLE 12. Periodicity of Draw Resonance (Shell)

Material	Draw Ratio V_L/V_0	Resonance period (s)	Resonance wavelength (cm)
HDPE-1	5.6	3.7	64
	5.8	3.7	66
HDPE-2	5.8	4.5	81
	6.2	4.6	88
	6.6	4.7	95
	6.8	4.8	100
HDPE-3	7.0	4.9	106
	10.7	4.3	142
	11.1	4.3	147
	11.5	4.4	156
	11.7	4.5	162
L-LDPE	9.3	4.3	123
	9.5	4.3	126
	9.7	4.3	128
	9.9	4.3	132
LDPE-1	10.1	4.35	136
	8.5	2.45	65
	11.2	2.6	91
	11.7	2.6	95
	12.0	2.65	99
LDPE-2	12.6	2.6	101
	23.2	2.5	182
	24.2	2.45	185
	25.2	2.5	197

Discussion

The results of the melt spinning experiments show the LDPE-1 and LDPE-2 to exhibit the most stable spinline and the HDPE-1 and HDPE-2 the least stable. The LDPE-2 is the most strikingly stable of all the materials investigated. The HDPE-3 and LLDPE are intermediate in their behavior.

Clearly the observations of the linear polymers indicate that spinline stability correlates with narrowness of molecular weight distribution. This agrees with the previous results of the Shell (Ref. 10) and APEC (Ref. 11,12) research teams on polypropylene. The long chain branched LDPEs are more stable than the linear polymers in agreement with our earlier study of polyesters (ref. 30). Minoshima (13) has reached similar conclusion to those cited above using a different set of linear branched (LDPE and LLDPE) polyethylenes.

TUBULAR FILM EXTRUSION

Results

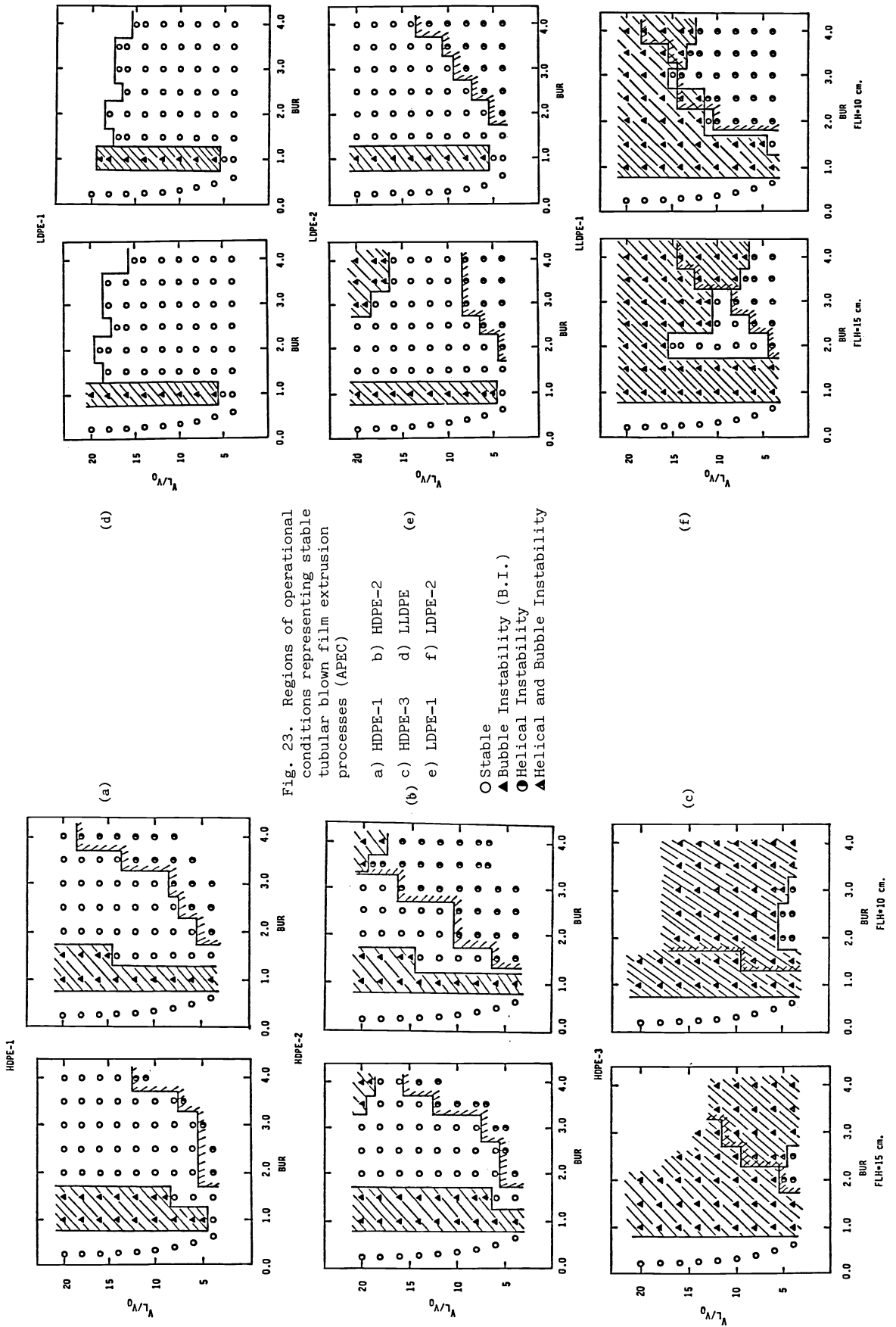
The stability of the tubular film process for the five polyethylenes was investigated by APEC. Following the procedure of Kanai and White (Ref. 16) and Minoshima (ref. 13) the regions of instability and stability are represented in a three dimensional space of draw-down ratio (V_L/V_0), blowup ratio (R_L/R_0), and frostline height (z_F). These three variables represent the kinematics of deformation of the bubble. In Fig. 23 a-f we display constant frostline height planes showing regions of stability and instability. It would appear that two different types of instability are observed. At a blowup ratio 1.0 and at a high (blow-up ratio) \times (draw down ratio) one finds the draw resonance type instability of Han and Park. At high blowup ratios one finds a bent and/or helically shaped bubble of the type described by Kanai and White (Ref. 16) and Minoshima (ref. 13).

It may be seen that HDPE-3 is the most unstable of all of the polymers. It has indeed no stable operating region. The LLDPE is only slightly better. The LDPE-1, LDPE-2, HDPE-1 and HDPE-2 have much broader regions of operating stability. Summarizing stability roughly orders as

$$\text{LDPE-1} > \text{LDPE-2} > \text{HDPE-1} > \text{HDPE-2} > \text{LLDPE} > \text{HDPE-3}$$

Discussion

The studies described above clearly indicate that LDPE-1 and LDPE-2 exhibit the most stable behavior. The HDPE-3 and LLDPE are the most unstable. The behavior is basically the same as that observed by Minoshima (ref. 13) on other polyethylene samples and similar to that of Kanai and White (ref. 16). The long chain branched LDPE polymers are the most stable followed by the broad molecular weight distribution HDPE. The narrow distribution HDPE and LLDPE are the most unstable.



The mechanisms for this variation must be primarily rheological in character. The behavior of the LDPEs are certainly related to the strain hardening elongational flow characteristics. The HDPEs all have the same activation energy at viscous flow. The LLDPE behaves like the HDPE-3 in which it is rheologically similar despite undoubtedly having a higher activation energy of viscous flow.

EXTRUSION INSTABILITIES

Results

BASF investigated the three HDPE melts at 190°C. In Fig. 24 extrusion pressure is plotted versus apparent shear rate. A steady extrusion pressure independent of the die cross section is observed for an L/D 60 die up to a critical shear rate $\dot{\gamma}$, which is indicated by the symbol \dagger . At higher shear rates a pulsation of the pressure is found. In that range no data points are given. The extrusion pressure becomes steady again above the shear rates marked by \ddagger . In that range the shear stress-shear rate behavior is dependent on the die cross section. This also implies the flow instability occurs at a critical shear rate of shear stress.

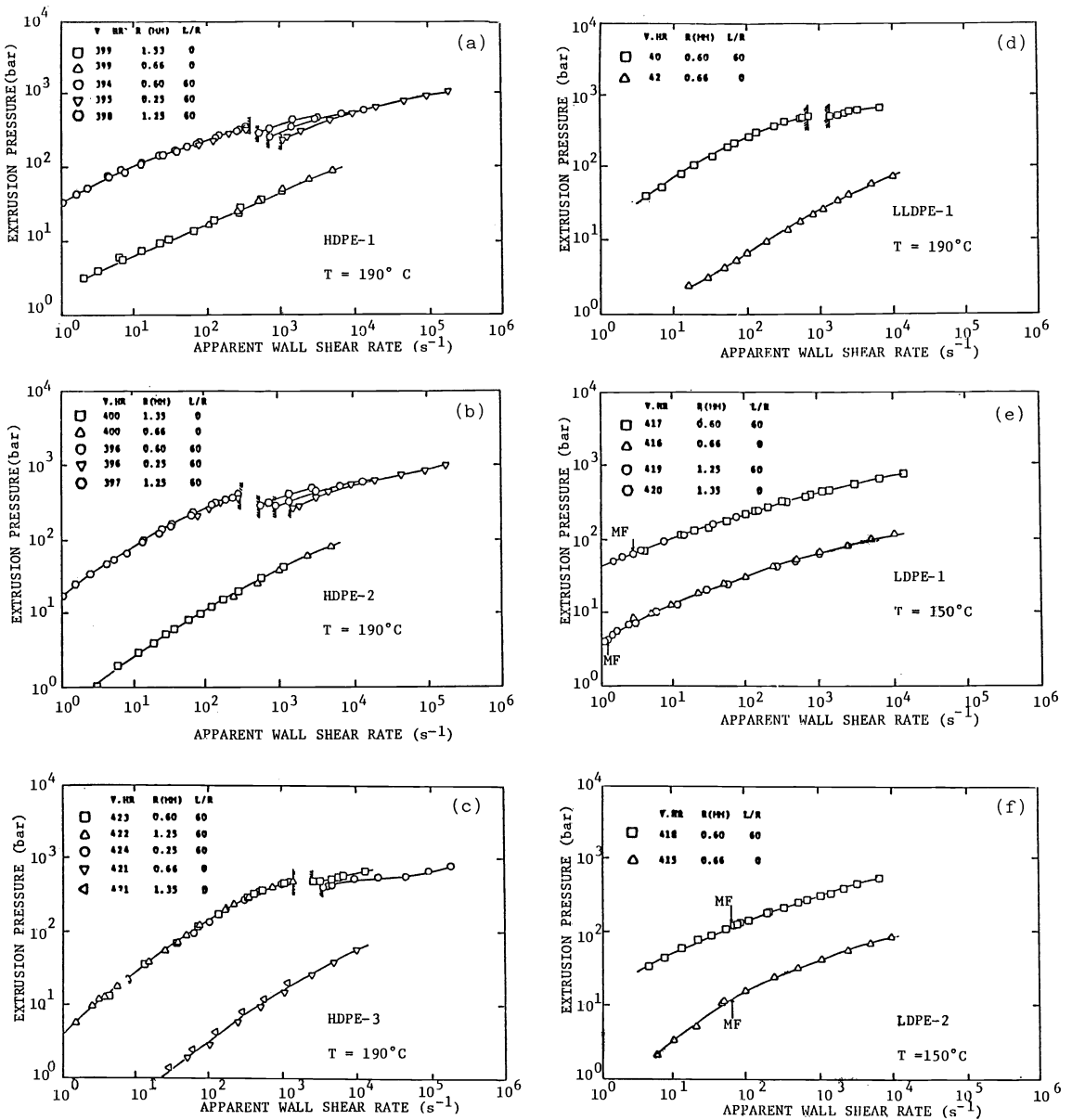


Fig. 24. Characteristic flow curves for polyethylene melts (BASF)

a) HDPE-1 b) HDPE-2 c) HDPE-3 d) LLDPE e) LDPE-1 f) LDPE-2

The LLDPE melt which was investigated at 190°C and 150°C exhibits a flow behavior which is very similar to that of the HDPE melts. Pulsation of the extrusion pressure is most pronounced at 150°C. The gap between the shear rates of steady extrusion pressure becomes broader with smaller diameter of the die.

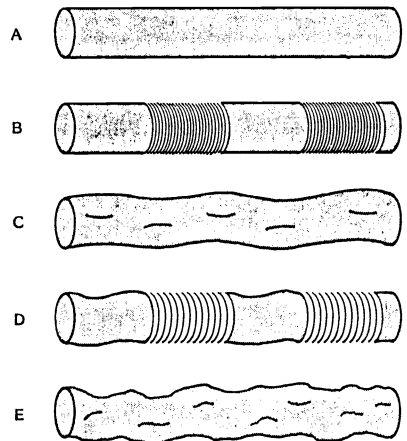
In the case of the two LDPE melts, which were investigated at 150°C, no oscillation of the pressure was found nor a dependence of the flow curve on the die cross section.

In Table 14, we compare critical die wall shear rates $\dot{\gamma}_w^*$ and shear stresses σ_w . The σ_w data unlike the shear rate is independent of temperature. The σ_w data is in the range of 0.5 to 5×10^5 pascal.

ETH observed that HDPE-3 and LLDPE exhibit two unstable flow regimes and not a single unstable regime like HDPE-1 and HDPE-2. The characteristics of the extrudate are shown in Fig. 25. The relationship of these extrudate shapes to positions on extrusion pressure apparent shear rate curves is shown in Fig. 26.

TABLE 14. Characterization of Extrusion Instabilities by BASF

Type	L/D = 30 D = 1.2mm Onset of Flow Instabilities		
	T [°C]	$\dot{\gamma}_w^* [s^{-1}]$	$\sigma_w [10^5 Pa]$
HDPE-1	190	395	2.6
HDPE-2	190	330	3.3
HDPE-3	190	1400	3.7
LLDPE	190	670	4.0
LLDPE	150	140	3.2
LDPE-1	150	285	0.48
LDPE-2	150	67	0.85



Extrudates of LLDPE and HDPE-3 at Different Extrusion Rates

Fig. 25. Characteristic flow curves for narrow MWD linear polyethylenes (ETH)

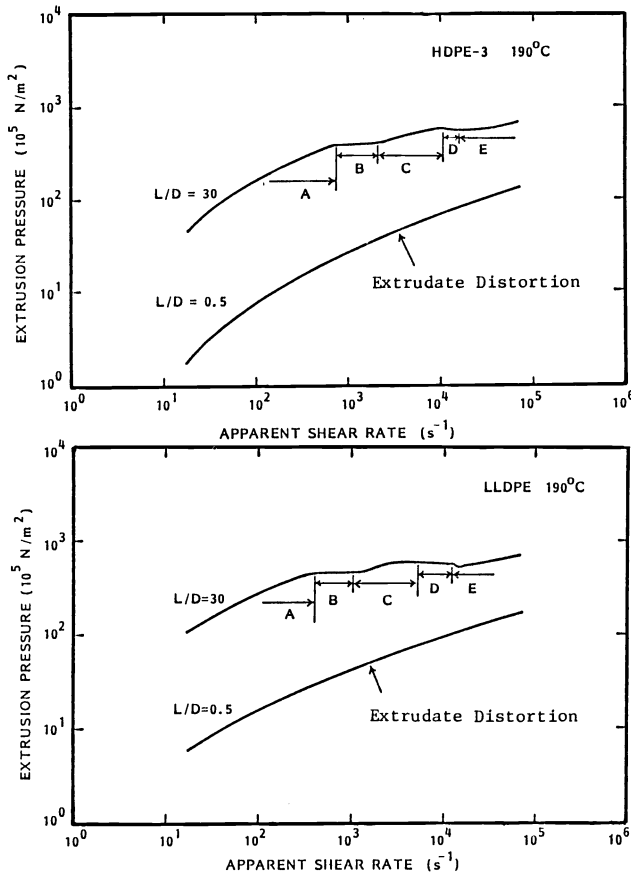


Fig. 26. Shapes of the extrudates of HDPE-3 and LLDPE at various extrusion rates (ETH)

CdFC who used a screw extruder, classified their observations according to:

- smooth : extrudate without any surface and diameter irregularities
- sharkskin : regular extrudate diameter by thread aspect
- melt fracture : extrudate with surface and diameter irregularities
- two zones : regular alternative zones of sharkskin and melt fracture

They present their data as die wall shear rate as a function of screw speed, using die diameter as a running parameter (see Fig. 27). Dotted lines delimit different visual aspect

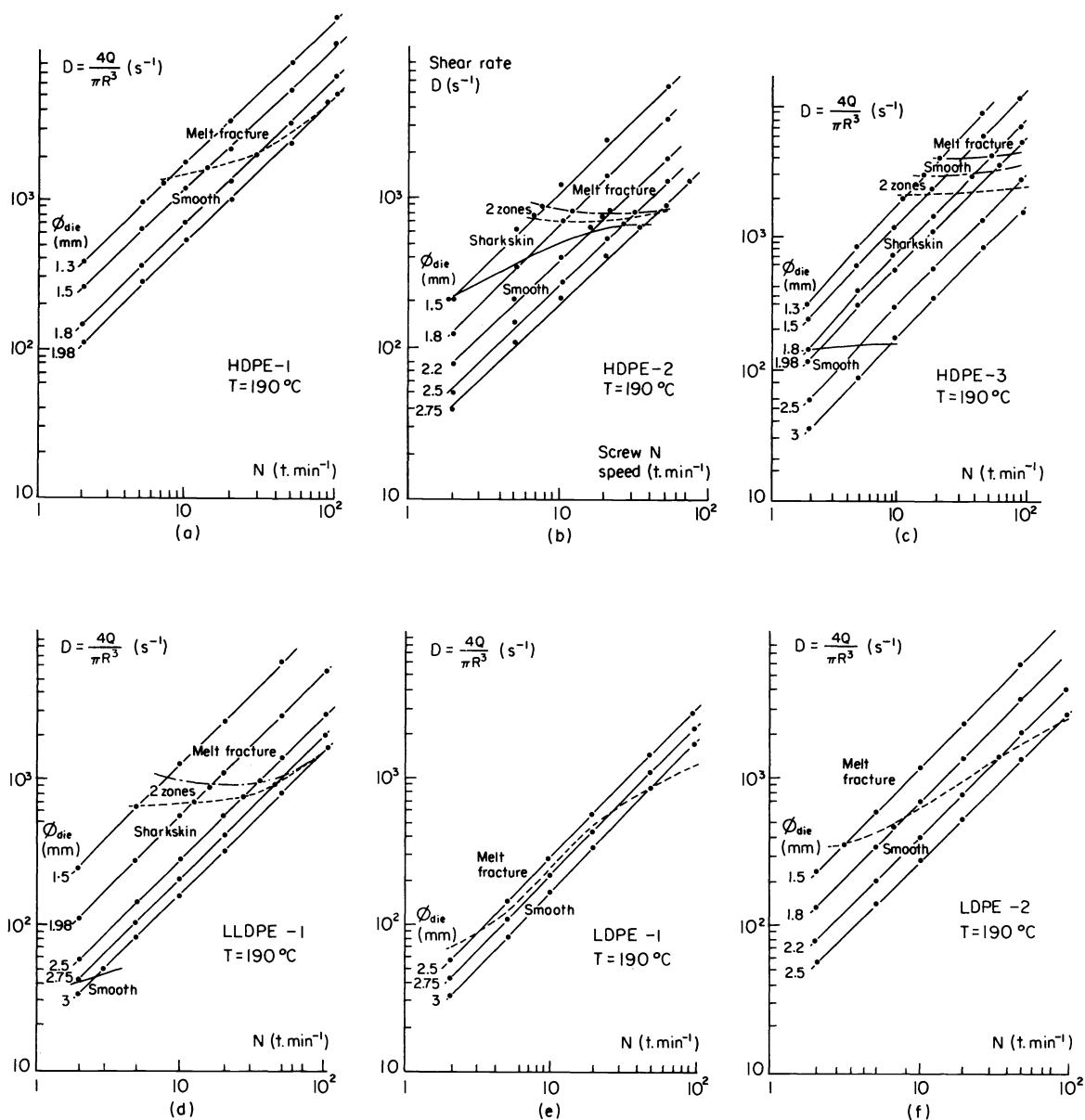


Fig. 27. Apparent shear rate $4Q/\pi R^3$ as a function of screw rotation speed of extruder for polyethylene melts (CdFC)

- a) HDPE-1 b) HDPE-2 c) HDPE-3
- d) LLDPE e) LDPE-1 f) LDPE-2

zones. There are differences between the five samples. We observe with increasing shear rate:

- smooth - sharkskin - two zones - melt fracture for one HDPE sample (HDPE-2) and for LLDPE 1; for HDPE-3 there is a supplementary smooth zone between 2 zones and melt fracture.
- direct modification from smooth extrudate to melt fracture for one HDPE sample (HDPE-1) and for the two LDPE samples.

Discussion

It is noteworthy that the three HDPE melts and LLDPE exhibit similar flow breakdown with inception of apparent slippage at about the same wall shear stress level i.e., $2.6\text{--}4.0 \times 10^5$ pascal and this probably the same mechanism. The LDPE breaks down at a lower shear stress $0.48\text{--}0.85 \times 10^5$ pascal apparently by a different mechanism. This corresponds to the observations of Tordella (ref. 23) more than a quarter century ago.

CONCLUSIONS

A series of linear polyethylenes of varying molecular weight distribution and extent of branching has been structurally and rheologically characterized in laminar shear flow and uniaxial extension. They have subsequently been investigated in a series of processing flows. Certain general conclusions may be reached classifying the stability behavior of the polymer melts in the different flows investigated. Specifically for uniaxial extension the stability as rated in terms of kinematic variables (stretch ratio) may be expressed as

LDPE-2 > HDPE-3 ~ LLDPE > LDPE-1 > HDPE-2 > HDPE-1

For melt spinning the critical drawdown ratios order as

LDPE-2 > LDPE-1 > HDPE-3 ~ LLDPE > HDPE-2 > HDPE-1

while for tubular film extrusion, the stability in terms of kinematics (drawdown ratio, blowup ratio) varies as

LDPE-1 > LDPE-2 > HDPE-1 ~ HDPE-2 > LLDPE > HDPE-3

For extrusion instabilities evaluated in terms of shear rate

HDPE-3 > LLDPE > HDPE-1 > HDPE-2 (190°C)

LDPE-1 > LLDPE > LDPE-2 (150°C)

and shear stress

HDPE-1 ~ HDPE-2 ~ HDPE-3 ~ LLDPE > LDPE-1 ~ LDPE-2

The rating in each case is different. Long chain branching seems generally stabilizing in elongational flows including uniaxial stretching, melt spinning and tubular film extrusion. Broadening molecular weight distribution in linear polymers is destabilizing for uniaxial stretching and melt spinning, but apparently stabilizing for tubular film extrusion.

PARTICIPATING MEMBERS AND LABORATORIES

Dr. H.M. Laun
BASF AG
D-ZKM-G201
D - 6700 Ludwigshafen/Rhein
Germany

Dr. S.T.E. Aldhouse
British Petroleum
P.O. Box 21
Bo'ness Road
Grangemouth, Stirlingshire FK 39XH
Scotland

Mr. H. Coster
Borg Warner Chemicals
P.O. Box 8122
Amsterdam
Netherlands

Dr. D. Constantin
Societe Chimique des Charbonnages
CdF Chimie
Centre de Recherches Nord
62160 Bully-Les-Mines
France

Dr. J. Meissner
Eidgenössische
Technische Hochschule Zurich
Technisches Laboratorium
Universitätsstrasse 6
CH - 8006 Zurich Switzerland

Dr. J.M. Starita
Rheometrics, Inc.
1 Possumkown Road
Piscataway
New Jersey 08854
USA

Dr. M. Fleissner
Hoechst AG
Kunststoff Forschung H
Postfach 80 03 20
D - 6230 Frankfurt am Main 80
Germany

Dr. Frank
Rheometrics GmbH
Arabella Center
Lyoner Strasse 44-48
D6000 Frankfurt aM. 71
West Germany

Dr. D.J. Groves
ICI Petrochemicals and Plastics Division
Wilton Centre
P.O. Box No. 90
Wilton
Middlesbrough
Cleveland
United Kingdom

Dr. G. Ajroldi
Montepolimeri SpA
Centre Recherche Bollate
Via S. Pietro, 50
I - 20021 Bollate
Italy

Dr. L.A. Utracki
National Research Council Canada
Industrial Materials Research Institute
75, Boul De Mortagne
Boucherville
Quebec
Canada

Pr. J.L. White
Dr. H. Yamane
Polymer Engineering Center
The University of Akron
Akron, Ohio 44325
USA

Mr. A. Ghijsels
Koninklijke/Shell Laboratorium
Postbus 3003
Badhuisweg 3
Amsterdam - N
Netherlands

Pr. H.H. Winter
Dept. of Chemical Engineering
University of Massachusetts
Amherst, Mass. 01003
USA

Acknowledgements

Research at the University of Akron was supported by the Division of Engineering of the National Science Foundation. The authors also wish to thank the efforts of Mr. Ho Jong Kang of the University of Akron.

REFERENCES

1. J. Meissner, Pure Appl. Chem. 42, 553 (1975).
2. H.H. Winter, Pure Appl. Chem. 55, 943 (1983).
3. Y. Ide and J.L. White, J. Appl. Polym. Sci. 20, 2511 (1976).
4. Y. Ide and J.L. White, J. Appl. Polym. Sci. 22, 1061 (1978).
5. W. Minoshima, J.L. White and J.E. Spruiell, Polym. Eng. Sci. 20, 1166 (1980).
6. H.I. Freeman and M.J. Coplan, J. Appl. Polym. Sci. 8, 2389 (1964).
7. S. Kase, T. Matsuo and Y. Yoshimoto, Seni Kikai Gakkaishi 19, 763 (1966).
8. A. Bergonzoni and A.J. DiCresci, Polym. Eng. Sci. 6, 45 (1966).
9. S. Kase, J. Appl. Polym. Sci. 18, 3279 (1974).
10. A. Ghijsels and J.J.S. Ente, Rheology Vol. 3, Edited by G. Astarita, G. Marrucci and L. Nicolais, Plenum, NY (1980).
11. W. Minoshima, J.L. White and J.E. Spruiell, J. Appl. Polym. Sci. 25, 287 (1980).
12. H. Yamane and J.L. White, Polym. Eng. Sci. 23, 516 (1983).
13. W. Minoshima, Ph.D. Dissertation in Polymer Engineering University of Tennessee, Knoxville (1983). Also W. Minoshima and J.L. White, J. Non. Newt. Fluid Mech. 19, 275 (1986).

14. C.D. Han and J.Y. Park, J. Appl. Polym. Sci. 19, 3291 (1975).
15. C.D. Han and R. Shetty, IEC Fund 16, 49 (1977).
16. T. Kanai and J.L. White, Polym. Eng. Sci. 24, 1185 (1984).
17. R.S. Spencer and R.E. Dillon, J. Colloid Sci. 4, 241 (1949).
18. J.P. Tordella, J. Appl. Phys. 27, 454 (1956).
19. J.P. Tordella, Rheol. Acta 1, 216 (1958).
20. P.L. Clegg, Trans. Plastics Inst. 28, 245 (1960).
21. E.B. Bagley and H.P. Schreiber, Trans Soc. Rheology 5, 341 (1961).
22. E.R. Howells and J.J. Benbow, Trans Plast. Inst. 30, 242 (1962).
23. J.P. Tordella, J. Appl. Polym. Sci. 7, 215 (1963).
24. H.M. Laun and H. Munstedt, Rheol. Acta 17, 415 (1978).
25. H. Yamane and J.L. White, Polym. Eng. Rev. 2, 167 (1982).
26. F.N. Cogswell, Polym. Eng. Sci. 12, 64 (1972).
27. T.G. Fox, S. Gratch and E. Loshaek in "Rheology" Vol. 1, Edited by F.R. Eirich, Academic Press, NY (1956).
28. G.V. Vinogradov and A.Y. Malkin "Rheology of Polymers" Mir, Moscow (1980).
29. C.D. Han and T.C. Yu, Rheol. Acta 10, 398 (1971).
30. K. Oda, J.L. White and E.S. Clark, Polym. Eng. Sci. 18, 25 (1978).
31. B.D. Coleman and H. Markovitz, J. Appl. Phys. 35, 1 (1964).
32. W.P. Cox and E.H. Merz, J. Polym. Sci. 28, 619 (1958).
33. J.L. White and H. Yamane, Pure Appl. Chem. 57, 1441 (1985).